

A model of surface fire, climate and forest pattern in the Sierra Nevada, California

Carol Miller ^{a,*}, Dean L Urban ^b

^a *Department of Forest Sciences, Graduate Degree Program in Ecology, Colorado State University, Fort Collins, CO 80523-2330, USA*

^b *School of the Environment, Duke University, Durham, NC 27708, USA*

Accepted 26 May 1998

Abstract

A spatially explicit forest gap model was developed for the Sierra Nevada, California, and is the first of its kind because it integrates climate, fire and forest pattern. The model simulates a forest stand as a grid of 15×15 m forest plots and simulates the growth of individual trees within each plot. Fuel inputs are generated from each individual tree according to tree size and species. Fuel moisture varies both temporally and spatially with the local site water balance and forest condition, thus linking climate with the fire regime. Fires occur as a function of the simulated fuel loads and fuel moisture, and the burnable area is simulated as a result of the spatially heterogeneous fuel bed conditions. We demonstrate the model's ability to couple the fire regime to both climate and forest pattern. In addition, we use the model to investigate the importance of climate and forest pattern as controls on the fire regime. Comparison of model results with independent data indicate that the model performs well in several areas. Patterns of fuel accumulation, climatic control of fire frequency and the influence of fuel loads on the spatial extent of fires in the model are particularly well-supported by data. This model can be used to examine the complex interactions among climate, fire and forest pattern across a wide range of environmental conditions and vegetation types. Our results suggest that, in the Sierra Nevada, fuel moisture can exert an important control on fire frequency and this control is especially pronounced at sites where most of the annual precipitation is in the form of snow. Fuel loads, on the other hand, may limit the spatial extent of fire, especially at elevations below 1500 m. Above this elevation, fuel moisture may play an increasingly important role in limiting the area burned. © 1999 Elsevier Science B.V. All rights reserved.

Keywords: Fire regime; Landscape pattern; Fire suppression; Spatial heterogeneity; Forest gap model

* Corresponding author. Present address: School of Forestry, University of Montana, Missoula, MT 59812, USA. Tel.: +1-406-5424187; fax +1-406-5424196; e-mail: cmiller/rmrs_missoula@fs.fed.us

1. Introduction

Of all the agents of landscape pattern formation, disturbance is perhaps the most striking, and fire is arguably the most well-studied large scale disturbance. Although the physics of fire behavior and spread (Rothermel, 1972) and the immediate effects of fire (e.g. Martin et al. 1979; Lotan et al., 1981) have been studied extensively, we know much less about how fires impact on ecosystem dynamics over longer time scales. One reason fire can be difficult to study is because it interacts with other factors across many scales. Two important factors interacting with fire regimes are climate and landscape pattern.

Climate primarily interacts with fire through its direct effect on fuel moisture. A short period of extreme fire weather can severely dry fuels, often overwhelming any effects that might be due to fuel loadings or fuel bed structure. But climate also affects the geographic distribution of vegetation types and site productivity, and, thus, indirectly influences the intensity, frequency and size of fires through the types of fuels that are made available and the rates at which those fuels accumulate. Over even longer time scales, climatic fluctuations are responsible for variations in fire regimes (e.g. Clark, 1988; Swetnam, 1993). An understanding of the relationship between climate and fire is especially critical because an important impact of climatic change on ecosystems will likely be via its effect on disturbance regimes (Overpeck et al., 1990).

The relationship between fire and vegetation pattern is important because fire simultaneously creates, and is influenced by, vegetation pattern. For example, the spread and behavior of fire in a closed canopy forest differs from that in an open woodland.

Model experiments also have demonstrated that there are qualitative differences in the spread of disturbance in fragmented versus connected landscapes, and forest mosaics may serve to stabilize landscapes with respect to fire (Turner et al., 1989, 1993; Turner and Romme 1994). Across North America, several decades of fire suppression may have altered the heterogeneity and connectivity of landscapes and consequently, the long term stability of forests.

The forests of the Sierra Nevada in California are ideal for studying these interactions among fire, climate and forest pattern. First, these forests are highly sensitive to climate. Vegetation composition is tightly coupled to the soil water balance (Stephenson, 1988; Urban et al., 1998), and paleoecological studies have revealed that vegetation has responded to past climatic changes (Davis et al., 1985; Anderson, 1990; Anderson and Carpenter, 1991). Second, frequent fires have created a forest mosaic, especially in the mixed conifer zone (Rundel et al., 1977). Decades of virtual fire exclusion have disrupted the natural fire regime, changed the structure and composition of these forests (Vankat and Major, 1978; Parsons and DeBenedetti, 1979), and may be responsible for the shift in the type and size of fires during the 20th century (Skinner and Chang, 1996). Finally, paleoecological evidence suggests that Sierra Nevada fire regimes are strongly influenced by climate (Swetnam, 1993; Caprio and Swetnam, 1995).

We have developed a new application of a forest gap model for the Sierra Nevada as part of the National Park Service's (now the USGS Biological Resources Division's) Global Change research initiative. One goal of this research initiative is to project how forest ecosystems might respond to climatic change. Fire is of special concern in the Sierra Nevada because climatic change is likely to affect fire regimes, which in turn will affect the condition of the forest. Within this model, we have integrated fire, climate, and forest pattern. This integration is rather new: neither landscape fire simulation models (e.g. Gardner et al., 1987) nor fire behavior models (Rothermel, 1972; Finney, 1994) have simulated vegetation dynamics with the detail that is afforded by gap models. Furthermore, most gap models that have incorporated fire (Keane et al., 1990; Kercher and Axelrod, 1984) have not integrated climate very well and cannot describe the spatial nature of fire or forest pattern. Although FIRE-BGC (Keane et al., 1996a,b) is a spatially explicit fire model that uses a forest gap model approach to simulate forest dynamics, it assumes forest stands are spatially homogeneous. Here, we are interested in the spatial pattern within forest

stands, and therefore have developed a model that simulates this pattern explicitly.

In this paper, we focus on fire as a major agent of pattern formation in the forests of the Sierra Nevada in California; we consider the physical environment and consequent biotic responses as agents of pattern formation in a companion paper (Urban et al., 1998). Here, we present the forest gap model and demonstrate its ability to couple the fire regime to both climate and forest pattern. In addition, we use the model to investigate the importance of climate and forest pattern as controls on the fire regime.

1.1. Study area

Our study focuses on Sequoia and Kings Canyon National Park, in the Sierra Nevada of California, USA (39° 35' N, 115° 35' W). The park encompasses a striking physical gradient, spanning 3500 m elevational relief over a distance of roughly 100 km. Vegetation ranges from foothill grassland and chaparral, through ponderosa pine, to the mixed conifer zone, to red fir and lodgepole pine, and finally to high-elevation pine near beeline (see key species names in Table 1). Vegetation types are distributed according to environmental conditions along elevation (tem-

perature and precipitation) and topographic-moisture gradients (Fig. 1).

Moisture status and fuel loads vary with forest condition and cause fire frequency to vary along these gradients. Generally, fire frequency increases toward drier environmental positions, and as fire frequency increases, fire severity tends to decrease (Fig. 1). Although lightning is most common at higher elevations (van Wagtenonk, 1993), its incidence can still be significant at lower elevations (Parsons, 1981). In the past, lightning ignitions at these lower elevations may have been augmented by an occasional fire that spread downslope from a higher elevation. Burning by native Americans before 1860, and by sheepherders during the late 1800s, also likely supplemented these lightning fires (Parsons, 1981). Prior to the 20th century, low elevation ponderosa pine forest stands experienced low intensity fires every 3–4 years (Warner, 1980). In the mixed conifer forest zone, low intensity surface fires burned through stands every 5–18 years (Kilgore and Taylor, 1979). Fires in the higher elevation red fir forests have been less frequent, with fire-free intervals for individual trees around 65 years (Pitcher, 1987). Mean fire return intervals are over 200 years in the sub-alpine forests, although evidence for fire exists in fire scarred trees and subfossil wood. Despite the high incidence of lightning, fuels are too discontinuous to sustain fires of any appreciable size at those elevations (Keifer, 1991).

Fire suppression since the early part of this century has disrupted the fire regime throughout the Sierra Nevada, allowing dead fuel to accumulate and understory tree density to increase in many forests (Vankat and Major, 1978). Forest managers recognize that frequent, low intensity fires historically reduced the likelihood of catastrophic wildfires. In an attempt to restore fire to some of these ecosystems, prescribed burning is currently used at low elevations and high elevation lightning fires are not suppressed (Agee, 1974; van Wagtenonk, 1991). Even so, the acres burned each year within the national parks falls well below that of historic levels (van Wagtenonk, 1993; Parsons, 1994).

Table 1
Tree species simulated by the model

Species code	Common name	Scientific name
ABCO	White fir	<i>Abies concolor</i> [Gord. and Glend.] Lindl. ex Hildebr.
ABMA	Red fir	<i>Abies magnifica</i> A. Murr.
CADE	Incense-cedar	<i>Calocedrus decurrens</i> [Torr.] Floren
PICO	Lodgepole pine	<i>Pinus contorta</i> Dougl. ssp. <i>murrayana</i> Grev. and Balf.
PIJE	Jeffrey pine	<i>Pinus jeffreyi</i> Grev. and Balf.
PILA	Sugar pine	<i>Pinus lambertiana</i> Dougl.
PIMO	Western white pine	<i>Pinus monticola</i> Dougl.
PIPO	Ponderosa pine	<i>Pinus ponderosa</i> Laws.
QUKE	California black oak	<i>Quercus kelloggii</i> Newb.

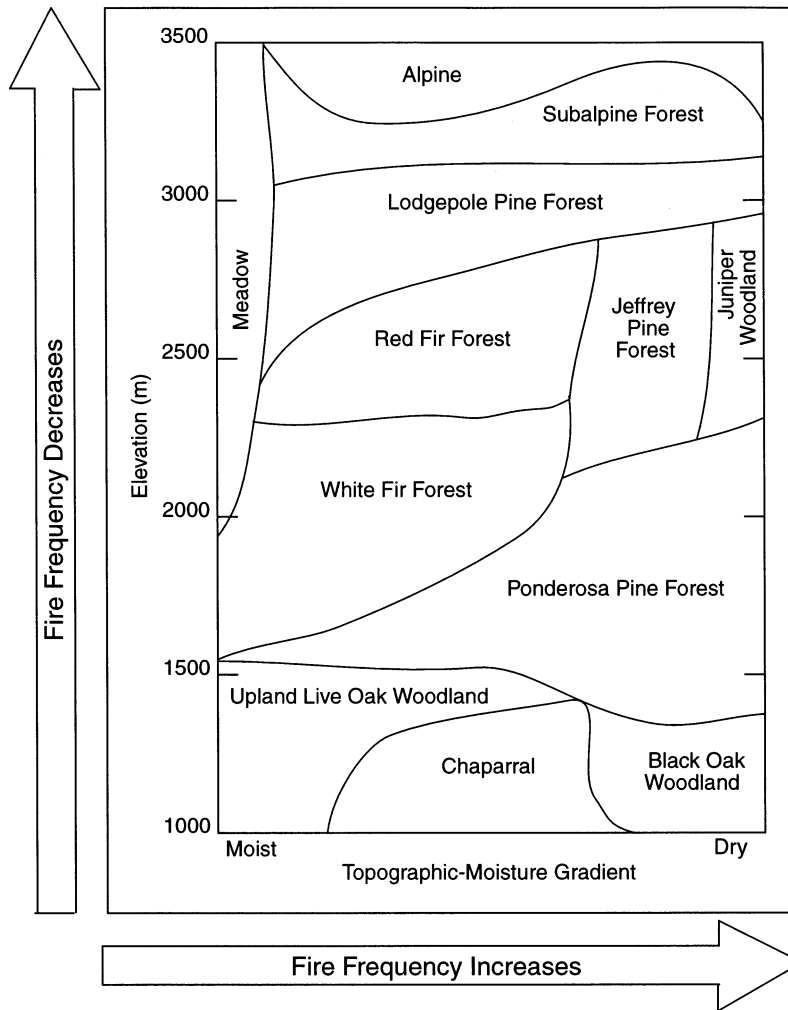


Fig. 1. The distribution of general vegetation types (redrawn from Vankat, 1982) and the relation of fire frequency to elevation and topographic-moisture gradients for Sequoia National Park, California.

2. Simulation model

To apply the forest gap model ZELIG (Urban and Shugart, 1992; Urban et al., 1993) to the Sierra Nevada, we expanded its soil water routine, parameterized it for Sierran mixed conifer species, and added a fire model. The new fire model is tightly coupled with the forest model through shared variables, arrays and functions. The forest model generates litter and woody debris that are defined in terms that can also be used in the fire model. As such, the decomposition and nutrient-cycling module of ZELIG is enslaved to the fire

model in this version. And the fire model depends on the soil water module in ZELIG for fuel moisture estimates, the model's crucial link to climate. Although the interdependency between the forest model and the fire model is considerable (Fig. 2), the fire model is distinct enough to be described separately. Descriptions of each follow.

2.1. Forest dynamics model

Because we have described the forest model in detail elsewhere (Urban et al., 1998), we provide only a brief treatment here. ZELIG simulates a

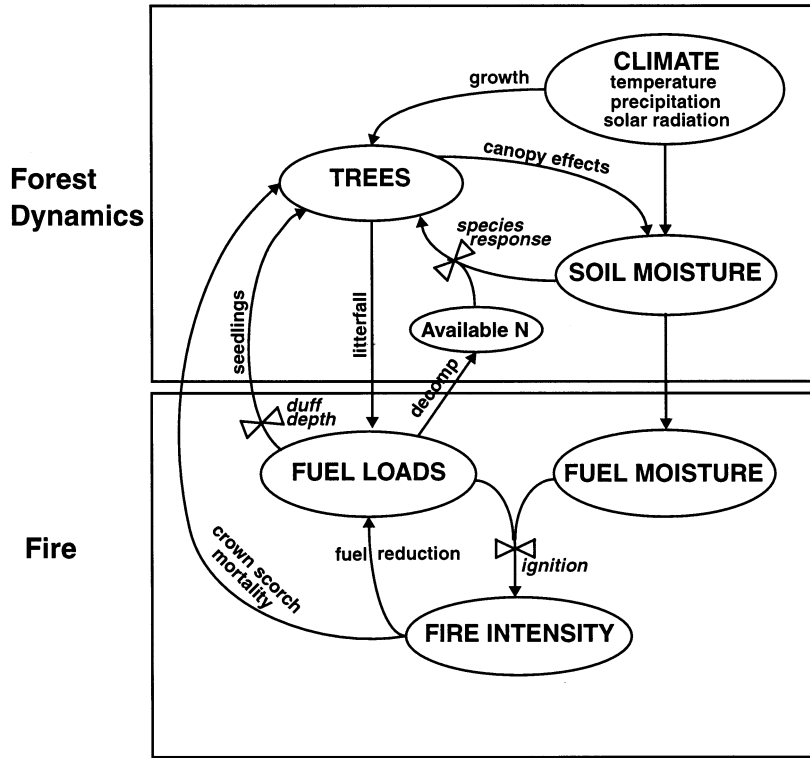


Fig. 2. Major interactions among the forest dynamics and fire submodels.

forest stand as a grid of 15×15 m forest plots. In this paper, we use a 20×20 grid to simulate a 9 ha forest stand. The grid is defined by elevation, slope and aspect. Elevation and topographic position are used internally by the model to adjust temperature and precipitation according to lapse rates (Running et al., 1987), and to adjust radiation (Nikolov and Zeller, 1992). The grid is underlain by a raster soil map so that each 15×15 m forest plot may have its own soil type. This version of the model contains an expanded soil water routine because of the critical role played by the soil water balance in these ecosystems.

2.1.1. The light regime

ZELIG uses allometric equations to estimate total leaf area for each tree on each plot. Leaf area is estimated from cross-sectional sapwood area at the base of live crown. Quadratic taper equations predict diameter (inside bark) at the base of live crown, d (Kozak et al., 1969):

$$d = D \sqrt{t_0 + t_1 \left(\frac{h}{H} \right) + t_2 \left(\frac{h^2}{H^2} \right)} \quad (1)$$

where D is diameter at breast height (dbh); t_0 , t_1 , and t_2 are regressed parameters given in Table 2; h is the height to the base of live crown; and H is total tree height. Total tree height is estimated as:

$$H = H_{\max} (1 - \exp(-h_2 D))^{h_3} \quad (2)$$

where H_{\max} is the typical maximum height in meters for a species; and h_2 and h_3 are coefficients listed in Table 2. Sapwood width is estimated as:

$$sw = s_0 (1 - \exp(-s_1 D)) \quad (3)$$

where s_0 and s_1 are coefficients given in Table 2. Sapwood width is assumed to be the same at crown base as at breast height. Sapwood cross-sectional area is computed by differencing heartwood area from total cross-sectional area.

Table 2
Constant parameters dimensioned by species

Name ^a	Parameter description	ABCO	ABMA	CADE	PICO	PIJE	PILA	PIMO	PIPO	QUKE
A_{\max}	Maximum age (year)	500	500	550	300	700	500	700	500	300
D_{\max}	Maximum diameter (cm)	200	200	200	100	200	200	100	200	100
H_{\max}	Maximum height (m)	70	70	50	50	60	70	60	65	30
dd_{\min}	Minimum growing degree-days	266	108	339	0	51	339	935	75	420
L	Shade tolerance (rank, 1 = intolerant)	4	4	3	2	2	3	3	2	1
M	Drought tolerance (rank, 1 = intolerant)	3	1	4	3	4	3	2	5	5
d_{lr}	Maximum duff for regeneration (cm)	99.9	99.9	99.9	2.5	5.0	5.0	2.5	5.0	99.9
$lyrs$	Number of lag years before planting at 2.5 cm dbh	5	5	5	5	5	5	5	5	5
h_2	Coefficient, height allometry	-0.0107	-0.0098	-0.0106	-0.0163	-0.0130	-0.0091	-0.0130	-0.0139	-0.0162
h_3	Coefficient, height allometry	1.023	1.058	0.945	1.163	1.228	0.957	1.228	1.141	0.706
t_0	Coefficient, taper equation	0.9690	0.9690	0.8507	1.1073	0.8519	0.8799	0.9090	0.9627	0.9758
t_1	Coefficient, taper equation	-1.6473	-1.6473	-1.7013	-1.2883	-1.4702	-1.4720	-1.4699	-1.3755	-1.2292
t_2	Coefficient, taper equation	0.6783	0.6783	0.8507	0.1811	0.6182	0.5922	0.4128	0.5610	0.2535
s_0	Coefficient, sapwood	4.7	4.7	4.7	18.2	15.1	15.1	15.1	15.1	15.1
s_1	Coefficient, sapwood	-0.0341	-0.0341	-0.0341	-0.0109	-0.0314	-0.0314	-0.0314	-0.0314	-0.0314
b_1	Coefficient, bark thickness	0.89	0.89	0.84	0.90	0.90	0.89	0.88	0.90	0.95
slr	Sapwood area: leaf area ratio	0.54	0.54	0.38	0.18	0.25	0.25	0.25	0.25	0.40
sla	Specific leaf area ($m^2 m^{-2}$)	6.1	6.1	7.1	7.0	7.0	7.0	7.0	7.0	12.6
f_{rt}	Foliage retention time (year)	6	7	4	3	4	4	3	2	1
bo_0	Coefficient, bole allometry	2.5512	3.4148	3.8627	4.5721	1.3088	2.4556	1.9919	2.4555	3.1998
bo_1	Coefficient, bole allometry	2.7856	2.7230	2.4454	2.3438	3.0037	2.7770	2.9260	2.7770	2.7242
bk_0	Coefficient, bark allometry	2.1069	2.3338	2.3854	1.0128	0.7473	2.1832	3.8845	2.1832	0.9848
bk_1	Coefficient, bark allometry	2.7271	2.5740	2.1987	2.0676	2.8858	2.6610	2.1677	2.6610	2.9890
bl_0	Coefficient, live branch	2.6718	2.6718	3.6417	2.3074	2.3330	-0.7293	2.3330	-0.7293	2.3288
bl_1	Coefficient, live branch	2.4300	2.4300	2.0877	2.3533	2.4645	3.3648	2.4645	3.3648	2.5760
bd_0	Coefficient, dead branch	4.7918	4.7918	3.3788	3.1109	4.3312	3.1109	4.3312	3.1109	-0.2162
bd_1	Coefficient, dead branch	1.0920	1.0920	1.7503	1.7426	1.4440	1.7426	1.4440	1.7426	2.8830
aw_0	Coefficient, aboveground wood	-3.2016	-2.7894	-2.3384	-2.1305	-3.9648	-3.9305	-3.9305	-3.1083	-3.3763
aw_1	Coefficient, aboveground wood	2.6528	2.6273	2.3420	2.3263	2.7513	2.8270	2.8270	2.6083	2.7242
tw_0	Coefficient, total wood	2.6119	2.5663	2.2797	2.2349	2.7252	2.7648	2.7648	2.5886	2.6475
tw_1	Coefficient, total wood	-2.9226	-2.3897	-1.9293	-1.5736	-3.7486	-3.5666	-2.9098	-3.5666	-2.9373

a Sources for parameter values: A_{\max} from Burns and Honkala (1990); D_{\max} , H_{\max} from J. Verner (US Forest Service, unpub. data); L , M from Minore (1979); t_0 , t_1 , t_2 , s_0 , s_1 , b_1 from S. Garman and P. Homann (Forestry Sciences Lab., Oregon State University, unpub. data); bo_0 , bo_1 , bk_0 , bk_1 , bl_0 , bl_1 , bd_0 , bd_1 , aw_0 , aw_1 , tw_0 , tw_1 from Gholz et al. (1979); slr from Waring et al. (1982) and Waring and Schlesinger (1985); sla from Dale and Hemstrom (1984); dd_{\min} , d_{lr} , $lyrs$ calibrated using Graber et al. (1993) and Stephenson (1988); f_{rt} calibrated using J. van Wagtenonk (USGS Biological Resources Division, unpub. data).

Sapwood area-to-leaf area ratios (slr, Table 2) are then used to compute leaf area.

ZELIG distributes this leaf area uniformly along each tree's live crown (after Leemans and Prentice, 1987). The leaf-area profile is used to estimate available light for each position (grid row, column, and height) within the model stand. ZELIG does this by partitioning light into direct-beam and diffuse-sky components, and sampling the forest canopy to estimate each component (Urban et al., 1991; Urban and Shugart, 1992). This approach allows a tree's influence to extend beyond a single grid cell; a small tree's influence is local to a single cell, but a tall tree may shade smaller trees several cells away. The available light and species shade tolerance (L , Table 2) are used to constrain seedling establishment and tree growth and to prune the lower canopy (Urban et al., 1998).

2.1.2. *The soil moisture regime*

Underlying the model grid is a soil map which assigns a soil type to each cell. A soil type is defined by a number of layers and each layer is defined by its depth and water-holding capacity (field capacity and wilting point). Bare rock can be specified as a soil with zero depth, thus having no water-holding capacity.

The soil water balance is a "tipping bucket" algorithm and is coupled to the light regime through the influence of radiation on evaporative demand. Water falls as rain, a portion is intercepted by the canopy, and throughfall, along with any snowmelt, infiltrates the top soil layer. The model uses a Priestley–Taylor estimate of potential evapotranspiration (PET) (Bonan, 1989) and uses leaf area to partition this between surface evaporation and transpiration. Surface evaporation is limited to the top soil layer while transpiration is apportioned over all soil layers (after Bonan, 1989). The canopy also governs interception of rainfall, and thus affects inputs to soil water. Therefore, although the model does not simulate transpiration explicitly, it is quite responsive to canopy development, and the soil water balance will vary for each grid cell according to local canopy conditions.

From the soil water content, the model computes two drought day indices (Pastor and Post, 1986). One index is computed over the top 20 cm of the soil profile and is used to regulate seedling establishment. A second index is integrated over the fine-root depth distribution over the entire soil profile and is used to modify growth of established trees. The drought day indices are used along with species drought tolerance (M , Table 2) to determine relative species drought response.

Litter and duff, the partially decomposed portion of foliage litter, together act as the top layer (O horizon) in the soil water routine. From the water content of this layer, a proxy for fuel moisture is calculated, as discussed below. Fuel moisture is an important variable in the fire model.

2.1.3. *Tree demographics*

The model simulates seedling establishment, annual diameter growth, and mortality for individual trees on each grid cell. Each of these demographic processes is specified as a maximum potential that can be achieved under optimal conditions. These potentials are then reduced to reflect suboptimal environmental conditions (e.g. low light or drought) on each simulated plot.

2.1.3.1. *Establishment.* ZELIG tracks age classes, or cohorts, of seedlings; the number of cohorts is defined by the number of lag years (lyrs, Table 2) before a seedling is established as a sapling. Each year, a new cohort is created by multiplying the maximum establishment rate by a regeneration multiplier for each species (Urban et al., 1998). This regeneration multiplier restricts seedling establishment according to available light at ground level and soil moisture status of the topsoil. Species may also be assigned a maximum litter depth (dlr, Table 2) in which they may germinate and establish. The cohort approach, although simplistic, introduces a timelag and allows stochastic weather events and fire to cull entire cohorts of seedlings before they are established in the model as individual saplings.

2.1.3.2. *Growth.* Optimal tree growth is simulated as an annual diameter increment that is a function

of leaf area, diameter, and tree height allometries. This optimal growth rate is restricted by available light, soil moisture, nutrients and temperature. The light and soil water regimes were described above.

To describe the nutrient status of each plot, the model computes a ratio of nitrogen supply to nitrogen demand. This ratio and species nutrient response class are used to constrain tree growth. Nitrogen supply in the model is generated from a constant annual input of nitrogen (a_{in} , Table 2) plus nitrogen released during decomposition of litter and woody debris. Decomposition pools coincide with the fuel size classes used in the fire model. As these fuels decompose, nitrogen is released according to the nitrogen content of each fuel class (p_n , Table 3). Nutrient demand is calculated by multiplying the expected annual increment of foliage, wood, and roots, by the nitrogen content of each tissue type (t_{nc} , Table 2). Tree growth is then constrained by available N via a relative ratio of supply to demand (bounded to [0, 1]). In the simulations discussed later, differential species response to nutrient availability is turned off to emphasize species responses to drought and fire.

The number of growing degree-days available for a site constrains tree growth and sorts out species abundance along temperature gradients with latitude or elevation. We calibrated degree-day curves to species distribution data in Sequoia National Park, improving upon the degree-day parabolas used in previous gap models (Urban et al., 1998). The curves used here are one-sided; only minimum growing degree-days (dd_{min} , Table 2) are used to restrict growth. In other words, we assume that trees may be sensitive to temperatures that are too cold, but at Sierra Nevada latitudes they are not sensitive to temperatures that are too warm in a physiological sense. Rather, we allow the “too warm” limit on species distributions to be created through temperature’s effect on evaporative demand (Urban et al., 1998).

2.1.3.3. Mortality. Trees may die for one of three reasons: age-related mortality, loss of vigor, or fire. Probability of age-related mortality is a func-

tion of the species-specific maximum age (A_{max} , Table 2); we assume that 1% of individuals growing under optimal conditions may survive to maximum age and that the mortality rate is constant with respect to age (Harcombe, 1987). Stress-related mortality results when trees are suppressed and are not growing vigorously. Individuals which have failed to achieve 10% of their potential growth increment, or an absolute diameter increment of 0.1 mm, for two or more consecutive years, are subjected to a mortality rate of 0.369; this rate reflects our assumption that 1% of stressed trees survive 10 years. Fire mortality is discussed below as a fire effect.

2.2. Fire model

The fire model links three major functions: fuel accumulation, fire occurrence and fire effects. In the model, the amount and moisture content of fuels determine if and how intensely a fire will burn. The fireline intensity (the rate of heat release along a unit length of fireline) is used to compute important fire effects, such as tree crown scorch.

2.2.1. Fuels

Fuel loadings and their accumulation rates are the crux of the fire model, as they influence both fire intensity and fire frequency. The environment and stand structure of each plot within the model grid affects the rates of fuel input and decomposition. Only “dead and down” fuels are treated by the fire model. These are classified by size according to conventions of fire behavior and fire danger models (Deeming et al., 1972): litter is freshly fallen foliage; 1-h time lag (1-HTL) fuels are woody materials less than 0.6 cm in diameter; 10-HTL fuels are 0.6–2.5 cm in diameter; 100-HTL are 2.5–7.6 cm in diameter; and 1000-HTL are larger than 7.6 cm in diameter. Duff represents the compact, partially decomposed layer of litter and is often referred to as the fermentation, or F layer. This layer is not considered important in fire behavior models (Burgan and Rothenmel, 1984), but it can influence seedling establishment and is stored in the model’s fuel array for convenience.

Table 3
Constant parameters used in the fire-related routines

Parameter name	Parameter description	Value	Source
fwtr	Fine wood turnover rate	0.15 year ⁻¹	Calibrated
fwf ₁	Fine wood fraction, 1-h wood	0.13 fraction	van Wagtenonk and Sydoriak (1987)
fwf ₂	Fine wood fraction, 10-h wood	0.35 fraction	van Wagtenonk and Sydoriak (1987)
fwf ₃	Fine wood fraction, 100-h wood	0.52 fraction	van Wagtenonk and Sydoriak (1987)
w	Windspeed	3.20 km h ⁻¹	Keane et al. (1990)
mext	Moisture of extinction	0.25 fraction	Keane et al. (1990)
bdd	Bulk density of duff	100.4 kg m ⁻³	Keane et al. (1990)
bdl	Bulk density of litter	31.7 kg m ⁻³	Keane et al. (1990)
fbulk	Bulk density of fuel bed	0.0216 kg m ⁻³	Rothermel (1972)
flt	Conversion of litter to duff	0.615 year ⁻¹	Calibrated
dk ₁	Decomposition of litter	0.42 year ⁻¹	Calibrated
dk ₂	Decomposition of duff	0.13 year ⁻¹	Calibrated
dk ₃	Decomposition of 1-h wood	0.42 year ⁻¹	Calibrated
dk ₄	Decomposition of 10-h wood	0.42 year ⁻¹	Calibrated
dk ₅	Decomposition of 100-h wood	0.42 year ⁻¹	Calibrated
dk ₆	Decomposition of 1000-h wood	0.16 year ⁻¹	Calibrated
pn ₁	Nitrogen content of litter	0.66%	P. Homann, Forestry Sciences Laboratory, Oregon State University (unpub. data)
pn ₂	Nitrogen content of duff	0.08%	P. Homann, Forestry Sciences Laboratory, Oregon State University (unpub. data)
pn ₃	Nitrogen content of 1-h wood	0.08%	P. Homann, Forestry Sciences Laboratory, Oregon State University (unpub. data)
pn ₄	Nitrogen content of 10-h wood	0.08%	P. Homann, Forestry Sciences Laboratory, Oregon State University (unpub. data)
pn ₅	Nitrogen content of 100-h wood	0.08%	P. Homann, Forestry Sciences Laboratory, Oregon State University, (unpub. data)
pn ₆	Nitrogen content of 1000-h wood	0.08%	P. Homann, Forestry Sciences Laboratory, Oregon State University (unpub. data)
ain	Annual nitrogen input	3.30 kg ha ⁻¹ year ⁻¹	P. Homann, Forestry Sciences Laboratory, Oregon State University (unpub. data), Stohigren (1988)
tmin	Total mineral content	0.055 fraction	Keane et al. (1990)
emin	Silica-free mineral content	0.011 fraction	Keane et al. (1990)
sigma ₁	Surface-to-volume ratio, litter	576.1 m ⁻¹	Brown (1972)
sigma ₂	Surface-to-volume ratio, duff	576.1 m ⁻¹	Brown (1972)
sigma ₃	Surface-to-volume ratio, 1-h wood	90.2 m ⁻¹	Brown (1972)
sigma ₄	Surface-to-volume ratio, 10-h wood	25.3 m ⁻¹	Brown (1972)
sigma ₅	Surface-to-volume ratio, 100-h wood	10.2 m ⁻¹	Brown (1972)
pdens	Particle density	10.5 m ⁻¹	Cohen and Deeming (1985)
lhv	Low heat value of fuel	5.16 kW kg ⁻¹	Cohen and Deeming (1985)

2.2.1.1. *Fuel inputs.* There are two types of input to the fuel bed: inputs from trees that die, and annual litterfall (needles and branches) from living trees. When a tree dies, the foliage mass is determined from leaf area, which is predicted from sapwood cross sectional area at the base of tree's live crown (Waring et al., 1982, Waring and

Schlesinger, 1985). Taper equations (Kozak et al., 1969) are used to predict the diameter at the base of the crown, which is then used to determine sapwood width and sapwood area. The mass of branch and bole wood is determined from allometric relationships (Gholz et al., 1979). We have assumed that all branch wood on trees less than

30 cm diameter at breast height (dbh) is less than 7.6 cm in diameter. This wood is subsequently divided into 1-, 10-, and 100-HTL fuel classes according to observed empirical fractions (fwf, Table 3). Any wood greater than 7.6 cm diameter comprises the 1000-HTL fuel class. For trees larger than 30 cm dbh, we have assumed that an increasing portion of branch wood (up to 40%) is from very large branches that are categorized as 1000-HTL. A future version of the model will improve this crude estimate and account for differences among species.

Large trees contain a huge amount of biomass, and adding this biomass as fuel in a single large pulse immediately after a tree dies produces unrealistic variability. Therefore, we meter woody fuel inputs from dead trees over approximately 40 years, a typical duration of a snag in many of these forests (Morrison and Raphael, 1993). Litter from tree foliage is metered over a shorter length of time: only 1% of the foliage is retained as long as 5 years. Our goal is not to simulate a population of snags, but rather to smooth out fuel input rates after tree death in a simple way. Future enhancements to the model could incorporate species- and size-specific lag times for snags.

Dead foliage from living trees is added to the litter pool as either a function of foliage retention time (frt, Table 2), or through pruning of the lower canopy in response to light limitation. Typical foliage inputs from living trees as a function of tree diameter are shown in Fig. 3. Species differences are due to differences in frt, and in practice, there is variability about these curves, reflecting the variation in leaf area among model plots.

Wood less than 7.6 cm in diameter (1-, 10- and 100-HTL fuels) is contributed to the fuel bed each year by living trees according to branch allometries and the fine wood turnover rate (fwtr, Table 3), and divided into appropriate fuel size classes using fwf (Table 3). The only 1000-HTL fuel inputs from living trees are branches that are greater than 7.6 cm in diameter; the proportion of these branches is determined in the same manner as described for dead trees. Annual woody fuel

inputs from living trees as a function of tree diameter are shown in Fig. 3. The differences in woody fuel inputs between pine and fir are due entirely to differences in allometries between the species (bl and bd, Table 2).

2.2.1.2. Decomposition. Each fuel class decays according to a constant rate (dk, Table 3). In addition to the decay rates for each fuel compartment is a rate for converting the structural portion of fresh litter to duff (fldt, Table 3) (Kercher and Axelrod, 1984). Each of the constant decay rates is modified by an abiotic decay multiplier, the product of temperature and soil moisture factors, calculated in ZELIG's weather and soil water routines. Therefore, as climate varies throughout a model run and water balance varies across the model grid, so do decomposition rates.

2.2.2. Fire occurrence

Fire events are simulated as a function of three factors: probability of fire, fuel load and fuel moisture. When a potential fire occurs, the fuel load and moisture of each plot on the grid define whether that plot is burnable and with what intensity fire burns. We do not explicitly simulate fire spread but instead simulate the burnable area that results from the spatially heterogeneous fuel bed conditions (Fig. 4).

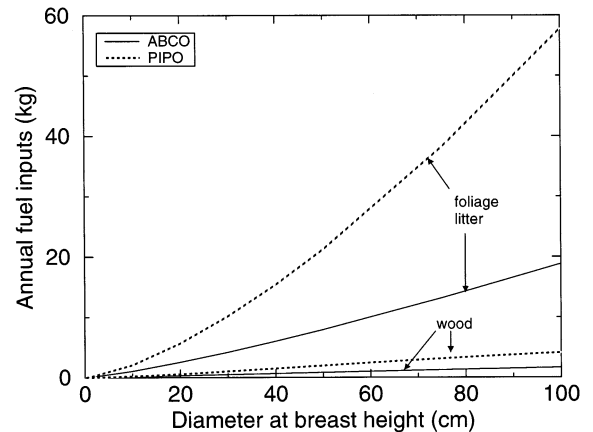


Fig. 3. Annual contribution of litter and woody fuels (less than 7.6 cm diameter) from live trees as a function of tree size and species.

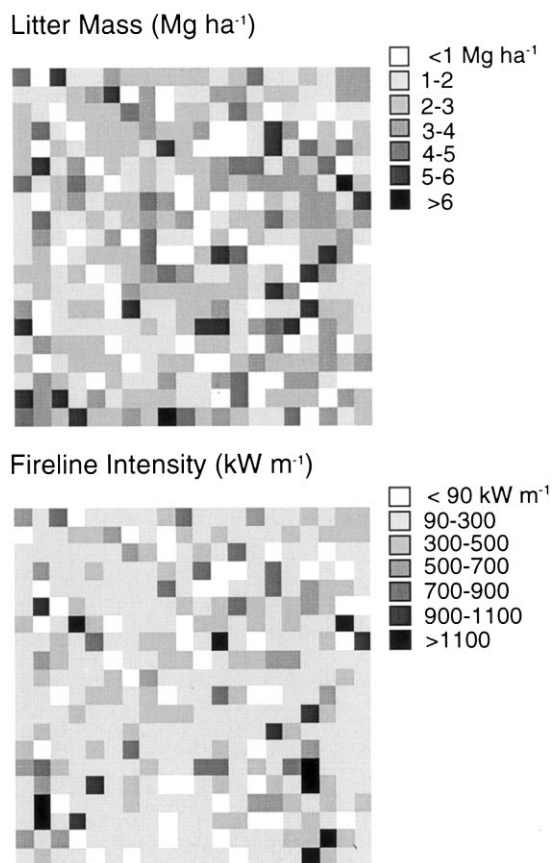


Fig. 4. The spatial pattern of (A) fuel loads (represented here by litter mass) and (B) fire intensity generated by the model. Each grid cell represents a 15×15 m plot within a 9-ha forest stand.

2.2.2.1. Fire interval. The mean ignition interval for potential fires for the model grid is specified at run time. The model uses this mean interval and draws uniform random numbers to generate stochastic fire events. For a given simulation year with a potential fire event, the month of fire occurrence is determined according to a seasonal fire occurrence distribution, also input at run time. A maximum of one fire event may occur in any year and each fire may spread to all cells within the model grid. For fire to occur, low fuel moistures and sufficient fuel loadings must also exist in addition to the stochastic fire event. Although simpler than the fire occurrence routine in FYRCYCL, which uses stochastically generated

fire weather patterns (van Wagtenonk, 1972, 1983), this method links climatic conditions (via fuel moisture) to fire occurrences.

2.2.2.2. Fireline intensity. If the current simulation year has an fire event, fire intensity is calculated for each plot, following equations for surface fire behavior developed by Rothermel (1972), and modified by Albini (1976). Fire intensity is largely a function of fuel loads and fuel moisture, but also depends on the following variables: moisture of extinction (m_{ext}), surface to volume ratio (σ), low heat value (lhv , mineral content (t_{min}), silica-free mineral content (e_{min}), particle density ($pdens$), bulk density ($fbulk$), wind speed (w), and slope. Constant values for these fuel parameters are given in Table 3. Neither duff nor 1000-HTL fuels are included in the calculation for fire intensity because these equations do not describe the smoldering combustion that occurs with duff, and are not able to treat the heterogeneity that occurs in large woody fuels such as bole wood (Rothermel 1983). Furthermore, these equations describe only surface fire behavior, and therefore, crown fires are not treated by the model.

Fuel moistures for each fuel size class are required for the fire intensity calculation, and these are derived from the duff moisture content. Equations for estimating these fuel moistures were derived from equations developed for the National Fire-Danger Rating System (Cohen and Deeming, 1985):

litter, 1-HTL fuel moisture

$$= (\text{duff moisture}/1.24)$$

10-, 100-HTL fuel moisture

$$= (\text{duff moisture}) * 1.19 \quad (4)$$

Duff moisture content is calculated monthly in ZELIG's soil water routine (Urban et al., 1998), with the duff layer treated as the top soil layer. This approach does not simulate short term fuel moisture dynamics. These estimates only represent average fuel moisture conditions, although they do reflect seasonal changes and interannual variation in weather.

Fire spread is not explicitly simulated, in the sense of characterizing a contagious process as a function of wind speed, wind direction and slope. We assume instead that fire instantaneously spreads to all plots. Certain plots may not have the proper conditions to sustain a sufficient fire, however; in those cases, the fire “burns out” and no fire effects are computed for that plot. In the model, fires burn out when fire intensity is less than 90 kW m^{-1} ; this intensity corresponds roughly to a scorch height of 1 m. Thus, a fire does not necessarily burn the entire model grid, and fire effects are calculated on a plot-by-plot basis. In reality, a single fire can burn for months, during which time fuel moisture and weather have changed many times, thus influencing fire behavior and fire severity. In the interest of emphasizing the effects of forest pattern on fire, we have simplified this reality considerably and simulate burnable area rather than actual fires.

2.2.3. Fire effects

Three fire effects are explicitly treated by the model: scorch height, tree mortality, and fuel reduction. Fuel reduction includes reduction of the duff layer, or forest floor, which can impact regeneration success in ZELIG’s regeneration routine.

2.2.3.1. Scorch height. Scorch height (m) is computed following Van Wagner (1973):

$$s = \frac{c_1 I^{(1.16667)}}{\sqrt{c_2 I + c_3 w^3 (t_{\text{kill}} - t_{\text{amb}})}} \quad (5)$$

where c_1 , c_2 and c_3 are constants with values $0.742 \text{ m } ^\circ\text{C}^{-1}$, $0.0256 (\text{ kW m}^{-1})^{4/3}$, and 0.278 h km^{-1} , respectively; I is fireline intensity (kW m^{-1}); w is wind speed (km h^{-1}); t_{kill} is lethal temperature, assumed to be 60°C ; and t_{amb} is ambient temperature ($^\circ\text{C}$), taken as the monthly mean temperature computed in ZELIG’s weather routine. The next version of the model will instead use mean daytime temperature for ambient temperature because most fire area is burned during the daytime. For surviving trees, the height to base of live crown is adjusted to scorch height, if necessary. Scorched foliage is added to the fuel bed as needlefall the following year. We have made the simplifying assumption that wind speed is a constant.

2.2.3.2. Fire mortality. Tree mortality due to fire is a function of percent of crown that is damaged, and cambial injury (Ryan and Reinhardt, 1988):

$$P_m = (1 + e^{(-1.94 + 6.32(1 - e^{b_{\text{thick}})}) + 0.000535c_{\text{kill}}^2}) - 1 \quad (6)$$

P_m is the probability of mortality in the year following the fire, b_{thick} is bark thickness (cm), and c_{kill} is percentage of the pre-fire crown volume killed. Bark thickness is determined from species-specific allometries (b_1 , Table 2). Percentage of the crown volume killed, c_{kill} , is determined from scorch height, live crown height and tree height (Ryan and Reinhardt, 1988):

$$c_{\text{kill}} = \frac{100(c_{\text{burn}}(2c_{\text{live}} - c_{\text{burn}}))}{c_{\text{live}}^2} \quad (7)$$

where C_{live} is the pre-fire live crown length (m) and C_{burn} is the length of the crown that was scorched (m). The probability of a tree dying depends on the volume of a tree’s crown that is killed; strictly speaking, this should reflect differences in morphology among species. We have not accounted for these differences, however, and instead assume that the shape of tree crowns among species is similar. Small trees are unlikely to survive most fires, as they are susceptible to high levels of crown scorch and have thin bark. Thus, fire has a significant effect on forest structure through the removal of these small trees.

2.2.3.3. Fuel reduction. Fuels are reduced by fire as a linear function of pre-fire fuel loading, while duff reduction is a function of duff moisture (Brown et al., 1985):

$$1\text{-, 10-HTL fuel}_{\text{post}} = 0.11(1\text{-, 10-HTL fuel}_{\text{pre}}) + 0.055$$

$$100\text{-HTL fuel}_{\text{post}} = 0.155(100\text{-HTL fuel}_{\text{pre}}) + 0.136$$

$$1000\text{-HTL fuel}_{\text{post}} = 0.21(1000\text{-HTL fuel}_{\text{pre}}) + 0.549$$

$$\text{duff}_{\text{post}} = \text{duff}_{\text{pre}}[(83.7 - 42.6 \text{ duff moisture})/100]. \quad (8)$$

Duff moisture is calculated monthly in ZELIG's soil water routine as a volumetric fraction of water content. After a fire, the reduction in fuels is partially offset by new fuels that originate from fire-killed trees; thus, under certain conditions post-fire fuel loads actually can be higher than pre-fire loads.

2.3. Parameterization

While the logic of this model is general, its parameterization is site-specific. Implementation of the forest model requires two sets of parameters: a site file and a species file. The site file consists of climate and soils data while the species file includes life-history traits, environmental responses, demographic rates and allometries. To invoke fire in the model, a third parameter file is required.

2.3.1. Site parameters

Climate data consist of lapse rates for mean minimum and maximum temperature for each month and for total monthly precipitation; we derived these from meteorological data from Sequoia National Park. Most soils in the mid-elevation mixed conifer zone of the Park are sandy loams of similar parent material and texture, and so we concentrated on using soil depth as the primary variable in our simulations. Finally, a turnover rate for tree branches (fwtr, Table 3) governs how much fine wood from each tree is contributed to the fuel bed each year. This parameter was calibrated to fuel accumulation data from Yosemite and Sequoia National Parks (van Wagtenonk, USGS Biological Resources Division, unpublished data; Parsons, 1978).

2.3.2. Species parameters

Species information and data were collated from a variety of sources, both local and regional (Gholz et al., 1979; Minore 1979; Burns and Honkala 1990; J. Verner, United States Forest Service, unpublished data; S. Garman and P. Homann, Forestry Sciences Laboratory, Oregon State University, unpublished data) and are listed in Table 2. For some parameters, we

lacked specific quantitative information for parameter estimation but had information with which we could rank differences among species (Minore, 1979). In such cases, we freed the parameters during calibration while keeping the estimates consistent with these accepted ranks. Also contained in the species file is the foliage retention time (frt, Table 2) which was calibrated for each species using litterfall data from Yosemite National Park (van Wagtenonk, USGS Biological Resources Division, unpublished data). In this paper, we have held tissue chemistry (pn, Table 3) equal across species to force the model to emphasize fire and soil water effects.

2.3.3. Fire parameters

A variety of values for fuel characteristics and other parameters are required by the fire-related functions in the model and were taken primarily from published data (Table 3). Decay rates for each fuel class were calibrated to fuel data from the Parks (Parsons 1978; van Wagtenonk and Sydoriak, 1987, van Wagtenonk, USGS Biological Resources Division, unpublished data). Also included in the fire file is a monthly frequency distribution that is used for stochastically determining the month in which fire occurs.

3. Model analysis

3.1. Simulations

To generate the appropriate model output for our evaluation of the model's performance, we conducted three series of simulations. All simulations were for Sequoia National Park (39.6°N, 115.6°W).

The first series tested the model's ability to simulate fuel accumulation rates. Fuel accumulation rates after fire are important because they can influence how soon the next fire might occur, and also how intense that fire might be. We ran 100-year simulations for three elevations (1650, 1850 and 2050 m), 18% slope and 212° aspect. This slope-aspect represents average conditions

for sites in Giant Forest in Sequoia National Park from a post-fire chronosequence study (Gebauer, 1992). Site elevations for the chronosequence spanned 1353–2340 m. We initialized the simulations with 500-year-old stand conditions that were previously generated by the model, and with post-fire fuel loads from the chronosequence study. Mean fuel loads were output each year during the simulations and compared to the independent fuel load data from the chronosequence.

In the second series, we assessed the model's ability to reproduce broad scale patterns in forest condition and fire regimes as these vary with elevation. We executed 300 model runs for a range of elevations and aspects, a range that encompasses the forested area of Sequoia National Park. Each simulation was 800 years; the first 700 years simulated a fire regime with a mean fire interval of 10 years, and the final 100 years simulated an era of fire suppression with no fire. We evaluated model output using two independent data sets: (1) we compared fuel loads and basal areas from the end of each run to plot data from Sequoia National Park (Graber et al., 1993; Stephenson, 1988); and (2) we compared summaries of fire frequency from each run to the fire scar record from an elevational transect in Sequoia National Park (Caprio and Swetnam, 1995). In addition, we used model output from these simulations to investigate the relative importance of fuel moisture and fuel load as each varies across this gradient.

The purpose of the third set of simulations was to examine the relationship between fire frequency and area burned. We executed model runs for each of five site descriptions corresponding to sequoia groves studied by Swetnam (1993). Each run was conducted for 200 years and was initialized with 500 year old stand data (generated from previous simulations). To obtain a range of fire frequencies, we varied the fire occurrence interval from 1 to 25 years. We then compared mean fire frequency and mean area burned at the end of each run to the fire scar data from these five giant sequoia groves (Swetnam, 1993).

3.2. Results

3.2.1. Fuels

The model's post-fire fuel accumulation compares well with the independent chronosequence data from Gebauer (1992) (Fig. 5). The species-specific values for foliage retention time (frit, Table 2) result in different accumulation rates at different elevations. For example, because ponderosa pine has the lowest value for frit and is most abundant in the 1650 m simulation, the 1650 m simulation shows the highest rates of litter and duff accumulation.

This model was designed to generate fuel loads that reflect forest condition. Consequently, fuel loads simulated by the model are strongly correlated with total basal area, because more trees in general, and larger trees in particular, generate more fuel. This relationship is apparent in the model output, as fuel loads track basal areas across the elevation gradient (Fig. 6). A similar relationship in the data set from Sequoia National Park (Graber et al., 1993; Stephenson, 1988) supports the relationship produced by the model.

3.2.2. Fire frequency

Fuel load and fuel moisture together influence whether a fire may burn, and therefore these factors influence the return interval for fires. Both of these factors vary with elevation in this model, and we expected that fire frequency would, as well. For our simulations, the model generated frequent fire at elevations below 2300 m (Fig. 7). Above this elevation, the model simulates higher moisture levels; consequently, fires are less frequent. This general pattern of decreasing fire frequency with elevation is also seen in the fire scar record for an elevational transect in Sequoia National Park (Caprio and Swetnam, 1995).

3.2.3. Fire frequency vs area burned

An inverse relationship between disturbance size or severity and disturbance frequency is thought to be an inherent feature of disturbance regimes (Pickett and White, 1985), and most

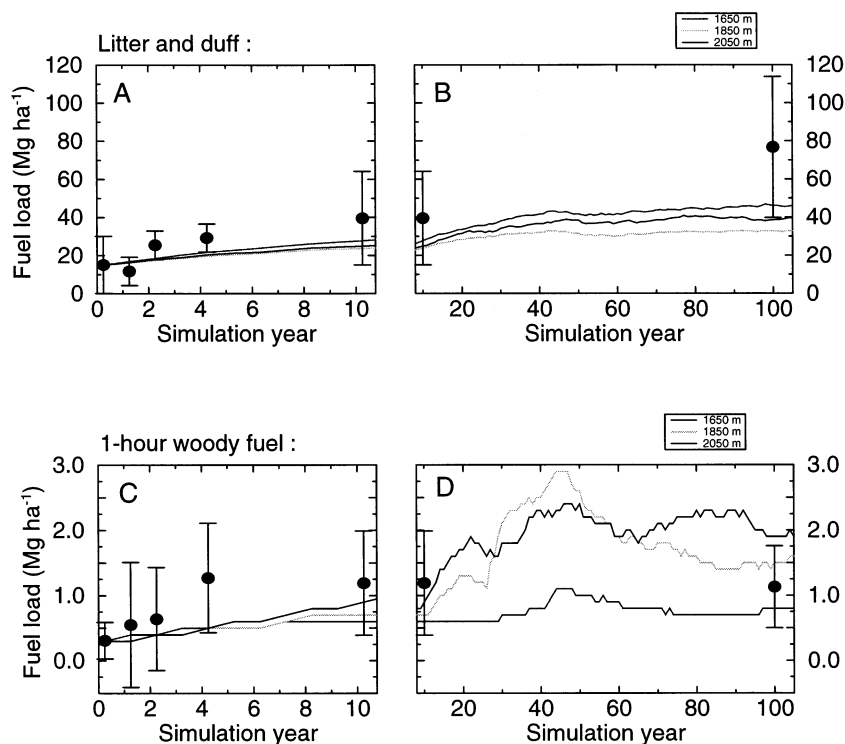


Fig. 5. Post-fire fuel accumulation rates. Litter and duff (combined) accumulation for (A) 10 years and (B) 100 years after fire. 1-h timelag woody fuel accumulation for (C) 10 years and (D) 100 years after fire. Filled circles with error bars represent data points from the chronosequence (Gebauer 1992), error bars are ± 1 S.D.; lines represent fuel loads (stand average) simulated by the model.

demonstrations of this relationship have used gross comparisons among different vegetation types (e.g. Heinselman, 1973). Swetnam (1993), however, analyzed this relationship within a single vegetation type. Fire scar records from five sequoia groves show a tendency for higher fire frequency periods to be dominated by apparently smaller fires, and lower frequency periods to have more widespread fires.

In the model, area burned is represented as the number of model plots that experience a fireline intensity greater than 90 kW m^{-1} . As shown in Fig. 8, mean area burned increases with mean fire interval because more fuels accumulate with more time between fires, thus generating more plots capable of supporting a fire. This relationship between area burned and fire frequency agrees quite well with the relationship derived from the fire scar record, although the model overestimates

the area burned relative to the fire scar data. The area burned predicted by the model may exceed the fire size inferred from the fire scar record because the model does not simulate contagious fire spread; in the model all plots with appropriate fuel bed conditions are burned even though they may not be connected in space. This is, of course, not representative of realistic fire spread. On the other hand, fire scar data may underestimate true fire size because not all fires will produce a fire scar on all trees. Thus, the discrepancy between the data and model output is exactly as we would expect.

3.2.4. Components of the fire regime

In simple terms, because fire converts fuel mass to energy, higher fuel loads should lead to more extreme fire behavior. But climatic factors and, consequently, the moisture content of fuels, can

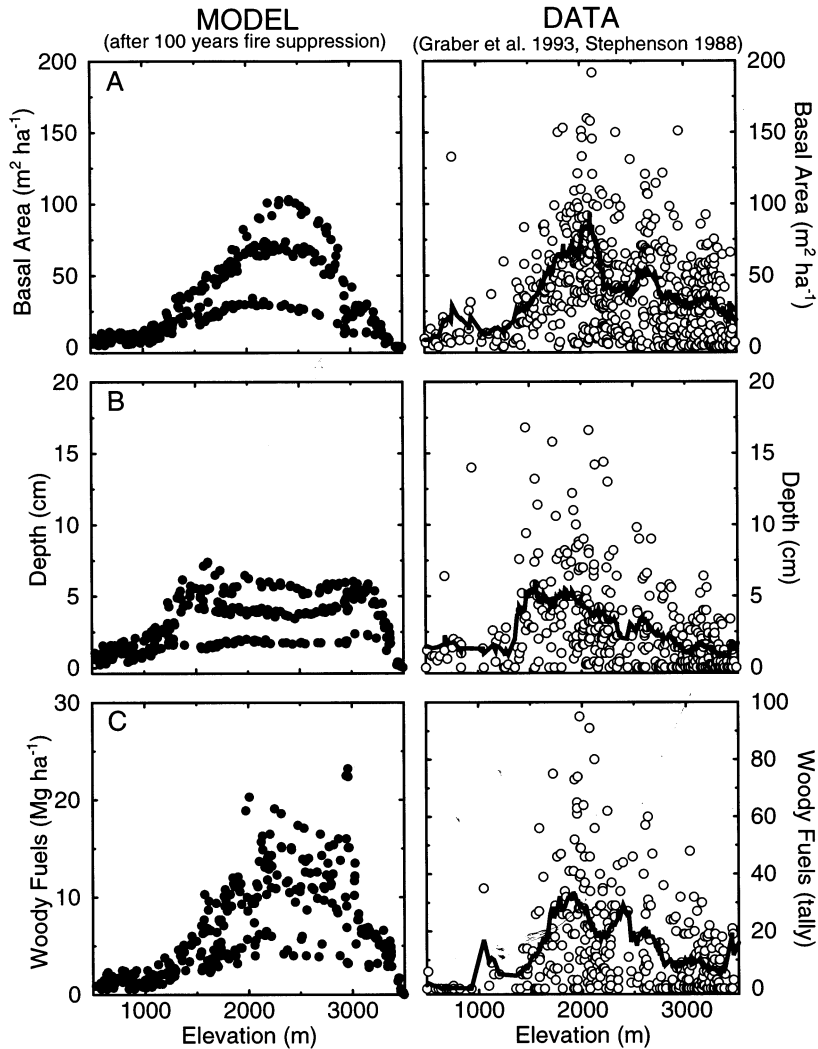


Fig. 6. Stand averages for (A) total basal area, (B) forest floor depth (litter and duff combined) and (C) fuel loads for woody fuels less than 7.6 cm diameter. Model results are shown as filled circles where each circle represents the final year value for a single simulation. The three distinct bands of points in the model output reflect different productivities that result from different topographic positions. Plot data from Sequoia National Park are shown as open circles on the right (Stephenson 1988; Graber et al. 1993). Forest floor depth is the average of measurements along a 10-m transect. Woody fuels also were tallied along these transects; the values are the total number of woody fuels encountered. Solid lines represent a 200-m running average.

overwhelm any effect that may result from the buildup of fuels. We analyzed model output to determine how the relative importance of fuel loads and fuel moisture varies across an elevational gradient, a gradient which correlates with both fuel productivity and climate. We compared the area of the model grid that burns with the

area that is dry enough to burn (Fig. 9). At elevations below 1500 m, almost the entire grid is dry enough for fire, yet only 20–45% of it burns. Fuel loads, therefore, limit the extent of burned area at these lower elevations. Above 1500 m, fuel loads begin to lose importance and fuel moisture plays a more important role in limiting the area

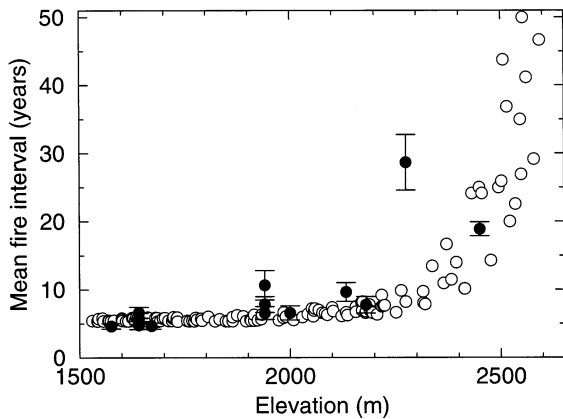


Fig. 7. Mean fire interval across the elevation gradient. Filled circles with error bars (± 1 S.D.) represent fire scar data for a transect through Sequoia National Park (Caprio and Swetnam 1995). Open circles represent simulations of 700 years of fires, using a fire occurrence interval of 5 years.

that can burn. Above 2300 m, increased variability in the burn:dry ratio results because some sites are fuel limited due to a short growing season which limits overall forest productivity. North facing slopes are less productive as well.

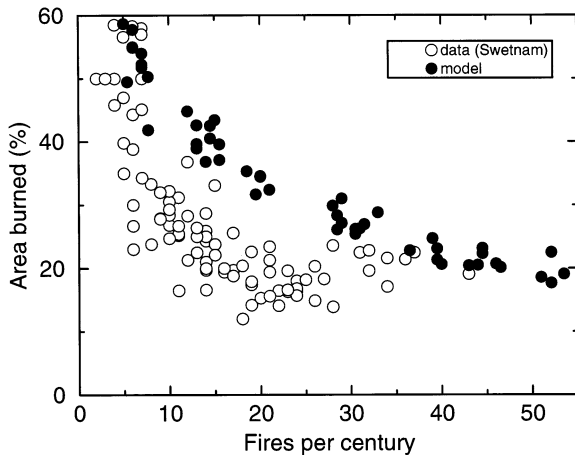


Fig. 8. Mean area burned related to fire frequency. Filled circles represent mean values from 200-year simulations; area burned is percent of model plots with simulated fire intensities greater than 90 kW m^{-1} . Open circles represent mean values from five giant sequoia groves, where area burned is percent of sample trees within a site having fire scars in the same year (Swetnam, 1993).

4. Discussion

This model has been parameterized for the mid-elevation forests of the Sierra Nevada but has a general structure that could be applied to other sites. The model uses the same two variables (fuel load and fuel moisture) to determine fire occurrence and fire intensity regardless of forest type. Furthermore, the coupling of fuels to tree-level allometries allows fuel loads to reflect an unlimited number of forest types. With the notable exceptions of the models FYRCYCL (van Wageningen, 1983), where fuel inputs are a function of basal area and species composition, and FIRE-BGC (Keane et al., 1996a,b), where fuel loads are generated from a dynamic carbon pool, most modeling approaches have assumed a constant fuel input rate for a given forest type (Kercher and Axelrod 1984; Keane et al., 1990). The ability to simulate fuel loads that reflect dynamic forest conditions is important because under a changing climate, forest condition and species assemblages may not resemble any “forest type” we know today (Betancourt 1990; Prentice 1992).

Surface fires consume dead and down fuel on the forest floor, as well as live herbaceous plants in the understory. Crown fires, on the other hand, spread through the canopies of live trees. This model was developed for surface fire regimes and assumes only dead and down woody fuels are important. For most forests in the Sierra Nevada, this is not a critical limitation, as crown fires are quite rare. To simulate ecosystems farther north, it is likely that we would have to include live fuels in the fire model. In addition, this could be a limitation at lower elevations in the Sierra Nevada where grasses are an important component of the fire regime. Model results suggest that fuel loads may limit the size of fires at elevations below 1500 m (Fig. 9), but grassy fuels could increase the connectivity of the fuel bed and the spatial extent of fires. We are currently adding herbaceous vegetation production to the model which will allow us to apply the model to lower elevations and to investigate the factors that influence the connectivity of fuels.

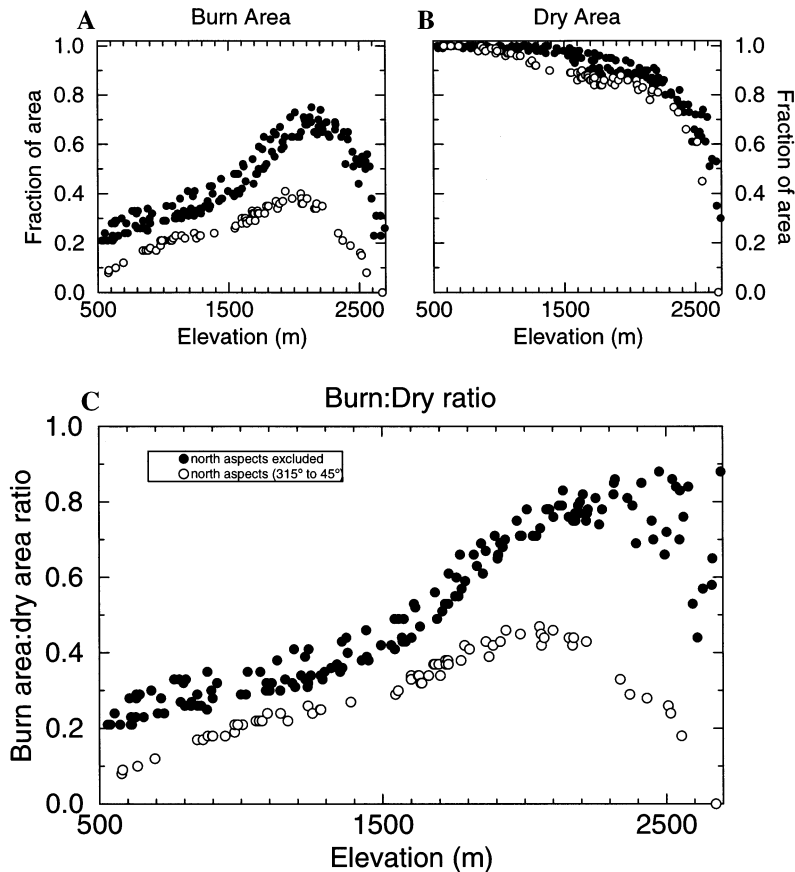


Fig. 9. The relative importance of fuel loads versus fuel moisture across the elevational gradient: (A) mean fraction of the grid that burns; (B) mean fraction of the grid that is dry enough to burn and (C) the ratio between these two mean areas. A ratio of 1 indicates that fuel moisture alone limits the area burned. A ratio of 0 indicates that fuel loads limit the size of the burned area. North-facing slopes (aspects 315°–45°), which experience a very different climatic regime than other aspects, are shown as open circles.

We simulate fuel moisture that varies both temporally and spatially with the local site water balance and forest condition. This enables the model to link climate with the fire regime which is an improvement over previous models. FYR-CYCL (van Wagendonk, 1983) also couples climate to the fire regime, but unlike gap models, it does not couple climate to vegetation dynamics. Gap models, on the other hand, have treated fuel moisture as a constant parameter (Kercher and Axelrod 1984; Keane et al. 1990). We do not attempt to link weather and fire, however. Soil water content, and thus fuel moisture, is estimated

using mean monthly values for precipitation and temperature. Therefore, effects from weather patterns that occur on time scales shorter than a month are not simulated by the model. Instead, effects from forest pattern are emphasized, which will be valuable for improving our understanding of the interaction between forest pattern and through the integration of climate, fire and forest response, this model can reproduce some important patterns of forest structure and fire regime. In our analysis of model performance, we have focused on its ability to reproduce patterns with elevation.

Elevation in the Sierra Nevada corresponds to a climatic gradient; precipitation increases while temperature decreases with elevation. This gradient strongly influences the water balance, the primary control on vegetation distribution (Stephenson 1988, 1990; Urban et al. 1998). The water balance also influences the fire regime. In the lower mixed conifer zone where ponderosa pine is dominant, highly flammable fuel is produced annually; given the proper moisture conditions, sufficient fuels usually exist to support a fire (van Wagtendonk, 1985). Proper moisture conditions are common at these low elevations in the Sierra Nevada and the result is frequent fire. In the upper mixed conifer forest, although the fuels necessary to support fire exist, the heavy snow-pack melts later in the season and fuels may not dry out until late summer (van Wagtendonk, 1985). The result is less frequent fire. In our simulations, we held fire occurrence probability constant across all elevations and it was the gradient in site water balance simulated by the model that was responsible for reproducing the trend of decreasing fire frequency seen in the fire scar record (Caprio and Swetnam 1995). This suggests that the moisture gradient is a sufficient explanation for the fire frequency pattern.

There are other factors which could interact with the moisture gradient to generate the fire frequency pattern but are not treated in this version of the model. Although fire frequency decreases with elevation, the frequency of lightning strikes actually increases (Vankat 1985; van Wagtendonk 1993). We will incorporate lightning frequency as a function of elevation in the next version of the model. Because the probability of lightning starting a fire at any particular location is very small, whether fire occurs can be very dependent on the fuel conditions in the surrounding landscape. In other words, fire frequency can be a function of the ease with which fire spreads throughout the surrounding landscape. Quantifying the ease with which fire spreads through a landscape is a difficult task, although it would be a fruitful avenue for future research.

The elevational pattern of fire frequency within the mixed conifer zone could be a result of the

bulk density of the fuel bed and its ability to carry a fire. As species composition shifts to short-needle fir with increasing elevation, the litter is more tightly packed and does not carry fire as readily as loosely packed long-needle pine litter. While this may play a contributing role to the pattern we see in the fire scar record, we do not feel it is the only explaining factor. White fir is clearly the forest dominant at elevations as low as 2000 m and would generate such a tightly packed litter layer, yet the fire scar record at those sites suggests high fire frequencies. It is more likely that the gradients in moisture, lightning frequency, ease of fire spread and bulk density interacted in the past to produce the observed pattern. We are currently including fuel bed bulk density as a function of species composition in the model (van Wagtendonk et al. 1998). In addition, we will update surface-to-volume ratios for woody particles and fuel particle densities using data for the Sierra Nevada species (van Wagtendonk et al., 1996).

Fire suppression has altered forest structure, increased fuel loads, and escalated potential fire hazard in the Sierra Nevada. The effect of fire suppression has been minor in those areas like the red fir zone, where fire occurrence is naturally restricted by short windows of suitable burning conditions. These areas experienced infrequent fires in the past and fire suppression does not represent a drastic departure from the historic fire regime (van Wagtendonk, 1993). In contrast, fire suppression has had the greatest effect in the mixed conifer zone. There, not only do fuels dry out early in the fire season, providing a wide window of opportunity for fire, but these highly productive forests have accumulated a lot of dead flammable fuel during decades of fire exclusion. Because our ability to suppress fires is not absolute, fires will eventually occur in these sites. Results from this model indicate that such sites may experience larger fires in the future than they have in the past (Fig. 8). Since 1972, Yosemite National Park has administered a program of prescribed natural fire, where lightning-ignited fires are allowed to burn under most conditions. For these lightning fires, van Wagtendonk (1993)

found that the white fir forest type has experienced more than twice as many large fires (fires greater than 400 ha) when compared with other vegetation types. The size distribution of fires in this zone may have been different before fire suppression; further analysis of these fires is needed to determine how fire suppression may have affected these fire size distributions.

A shift in relative importance between fuel moisture and fuel loads in limiting area burned appears to occur in the heart of the mixed conifer forest. Consequently, while the mid and low elevation forests may be most susceptible to the impacts of fire suppression, the higher elevations may be more vulnerable to climatic change. Our results suggest that high fuel moistures play an increasingly important role in limiting burnable area above 1500 m elevation. Global warming, more frequent droughts, or changes in the distribution of precipitation throughout the year, could push fuel moistures below a critical threshold and qualitatively alter the fire regime at these elevations. Such a change in the fire regime could have profound consequences for the condition and character of the forest.

The model's treatment of species-specific responses to fire can be improved. The fire mortality equations were developed for Rocky Mountain forests; some of these may not be appropriate for the Sierra Nevada. We are currently incorporating new equations developed for Sierran species (Stephens, 1995). Another important effect of fire is to reduce forest floor depth, thereby allowing the regeneration of certain species. As part of a seedling demography study, forest floor depth was measured so that it could be correlated with seedling survival (R. Kern, Duke University, unpublished data). These data are not yet available, but this is an area of the model that can be improved to better represent species responses to fire.

5. Conclusions

The interactions among climate, fire and forest pattern in the Sierra Nevada are complex: climate

controls fire frequency, fire affects forest pattern, and forest pattern influences aspects of the fire regime. We have developed a spatially explicit model to examine these interactions across a wide range of environmental conditions and vegetation types. The model performs well in several areas. Patterns of fuel accumulation, climatic control of fire frequency and the influence of fuel loads on the spatial extent of fires in the model are well-supported by data. The model shows great potential in its ability to generate within-stand spatial heterogeneity in forest condition, fuel loads and fuel moisture. With this feature, we are now able to examine how forest pattern and connectivity of fuels interact with changes in surface fire regimes.

We developed this model as a tool for learning about Sierra Nevada forests. Enhanced understanding of how these forests respond to long term changes in climate and fire regimes will be extremely useful for land managers in the Sierra Nevada. In the model, the two controlling factors that describe the climate-fire-forest system in the Sierra Nevada are fuel moisture and forest productivity (as it affects fuel loads), both of which are strongly influenced by the water balance. Model results suggest that fuel moisture exerts an important control on fire frequency, and that this control is especially pronounced at sites where the majority of annual precipitation is in the form of snow. In addition, our simulations suggest that fuel loads may limit the spatial extent of fire below 1500 m and that fuel moisture may start to limit the area burned above this elevation. If this is true, the area burned could increase in lower elevation forests as a result of fire suppression while the area burned in higher elevation forests may be sensitive to climatic change.

Acknowledgements

Funding for this research was provided by the Global Change Research Program, USGS, Biological Resources Division. We thank Jan van Wagtenonk, Nate Stephenson, Chiru Chang and anonymous reviewers for helpful comments on earlier drafts. Discussions with Dave Parsons,

Tom Swetnam, and all other collaborators on the Sierra Nevada Global Change Research Program who also have contributed greatly to this manuscript.

References

- Agee, J.K., 1974. Fire management in the national parks. *West. Wildlands* 1, 27–33.
- Albini, F.A., 1976. Estimating wildfire behavior and effects. USDA For. Serv. Gen. Tech. Rep. INT-30.
- Anderson, R.S., 1990. Holocene forest development and paleoclimates within the central Sierra Nevada, California. *J. Ecol.* 78, 470–489.
- Anderson, R.S., Carpenter, S.L., 1991. Vegetation change in Yosemite Valley, Yosemite National Park, California, during the protohistoric period. *Madrono* 38, 113.
- Betancourt, J.L., 1990. Late quaternary biogeography of the Colorado plateau. In: Betancourt, J.L., Van Devender, T.R., Martin, P.S. (Eds.), *Packrat Middens: the Last 40000 Years of Biotic Change*. University of Arizona Press, Tucson, pp. 259–292.
- Bonan, G.B., 1989. A computer model of the solar radiation, soil moisture, and soil thermal regimes in boreal forests. *Ecol. Model.* 45, 275–306.
- Brown, J.K., 1972. Field test of a rate-of-fire-spread model in slash fuels. USDA For. Serv. Res. Paper INT-116.
- Brown, J.K., Marsden, M.A., Ryan, K.C., Reinhardt, E.D., 1985. Predicting duff and woody fuel consumed by prescribed fire in the northern Rocky Mountains. USDA For. Serv. Res. Paper INT-337.
- Burgan, R.E., Rothermel, R.C., 1984. BEHAVE: fire behavior prediction and fuel modeling system-FUEL subsystem. USDA For. Serv. Gen. Tech. Rep. INT-167.
- Burns, R.M., Honkala, B.H., 1990. *Silvics of North America: I. Conifers*. Agriculture Handbook 654. USDA For. Serv. Washington, D.C. vol. 1, 675 p.
- Caprio, A.C., Swetnam, T.W., 1995. Historic fire regimes along an elevational gradient on the west slope of the Sierra Nevada, California. In: Brown, J.K., Mutch, R.W., Spoon, C.W., Wakimoto, R.W. (Tech coord.). *Proc. Symp. Fire in Wilderness and Park Management*, Missoula, MT, March 30–April 1, 1993, pp. 173–179.
- Clark, J.S., 1988. Effect of climate change on fire regimes in northwestern Minnesota. *Nature* 334, 233–235.
- Cohen, J.D., Deeming, J.E., 1985. The national fire-danger rating system: basic equations. USDA For. Serv. Gen. Tech. Rep. PSW-82.
- Dale, V.H., Hemstrom, M., 1984. CLIMACS: a computer model of forest stand development for western Oregon and Washington. USDA For. Serv. Res. Paper PNW-327.
- Davis, O.K., Anderson, R.S., Fall, P.L., O'Rourke, M.K., Thompson, R.S., 1985. Palynological evidence for early Holocene aridity in the southern Sierra Nevada, California. *Quat. Res.* 24, 322–332.
- Deeming, J.E., Lancaster, J.W., Fosberg, M.A., Furman, R.W., Schroeder, M.J., 1972. National fire-danger rating system. USDA For. Serv. Res. Paper RM-84.
- Finney, M.A., 1994. Modeling the spread and behavior of prescribed natural fires. In: *Proceedings of the 12th Conference on Fire and Forest Meteorology*. Jekyll Island, GA, October 26–28, 1993, pp. 138–143.
- Gardner, R.H., Milne, B.T., Turner, M.G., O'Neill, R.V., 1987. Neutral models for the analysis of broad-scale landscape patterns. *Landscape Ecol.* 1, 19–28.
- Gebauer, S.B., 1992. Changes in soil properties along a post-fire chronosequence in a sequoia-mixed conifer forest in Sequoia National Park, California. M.S. Thesis. Duke University, Durham, North Carolina.
- Gholz, H.L., Grier, C.C., Campbell, A.G., Brown, A.T., 1979. Equations and their use for estimating biomass and leaf area of plants in the Pacific Northwest. For. Res. Lab., Oregon State University, Corvallis. Res. Paper 41.
- Graber, D.M., Haultain, S., Fessenden, J.E., 1993. Conducting a biological survey: a case study from Sequoia and Kings Canyon National Parks. In: Veirs, Jr., S.D., Stohlgren, T.J., Schonewald-Cox, C. (Eds.), *Proc. 4th Conf. Research in California's national parks*. Trans. Proc. Ser. 9. US Dept. of the Interior, National Park Serv., pp. 17–35.
- Harcombe, P.A., 1987. Tree life tables. *BioScience* 37, 557–568.
- Heinselman, M.L., 1973. Fire in the virgin forest of the Boundary Waters Canoe Area, Minnesota. *Quat. Res.* 3, 329–382.
- Keane, R.E., Arno, S.F., Brown, J.K., 1990. Simulating cumulative fire effects in ponderosa pine/Douglas-fir forests. *Ecology* 71, 189–203.
- Keane, R.E., Morgan, P., Running, S.E., 1996a. FIRE-BGC: a mechanistic ecological process model for simulating fire succession on coniferous forest landscapes of the northern Rocky Mountains. USDA For. Serv. Res. Paper INT-484.
- Keane, R.E., Ryan, K.C., Running, S.W., 1996b. Simulating effects of fire on northern Rocky Mountain landscapes with the ecological process model FIRE-BGC. *Tree Physiol.* 16, 319–331.
- Keifer, M., 1991. Age structure and fire disturbance in the southern Sierra Nevada subalpine forest. M.S. thesis. University of Arizona, Tucson.
- Kercher, J.R., Axelrod, M.C., 1984. A process model of fire ecology and succession in a mixed-conifer forest. *Ecology* 65, 1725–1742.
- Kilgore, B.M., Taylor, D., 1979. Fire history of a sequoia-mixed conifer forest. *Ecology* 60, 129–142.
- Kozak, A., Munro, D.D., Smith, J.H.G., 1969. Taper functions and their application in forest inventory. *For. Chron.* 45, 278–283.
- Leemans, R., Prentice, I.C., 1987. Description and simulation of tree-layer composition and size distribution in a primaeval Picea-Pinus forest. *Vegetatio* 69, 147–156.

- Lotan, J.E., Alexander, M.E., Arno, S.F., French, R.E., Langdon, O.G., Loomis, R.M., Norum, R.A., Rothermel, R.C., Schmidt, W.C., van Wagtenonk, J.W., 1981. Effects of fire on flora. USDA For. Serv. Gen. Tech. Rep. WO-16.
- Martin, R.E., Anderson, H.E., Boyer, W.D., Dieterich, J.H., Hirsch, S.N., Johnson, V.J., McNab, W.H., 1979. Effects of fire on fuels. USDA For. Serv. Gen. Tech. Rep. WO-13.
- Minore, D., 1979. Comparative autecological characteristics of northwestern tree species—a literature review. USDA For. Serv. Gen. Tech. Rep. PNW-87.
- Morrison, M.L., Raphael, M.G., 1993. Modeling the dynamics of snags. *Ecol. Appl.* 3, 322–330.
- Nikolov, N.T., Zeller, K.F., 1992. A solar radiation algorithm for ecosystem dynamic models. *Ecol. Modell.* 61, 149–168.
- Overpeck, J.T., Rind, D., Goldberg, R., 1990. Climate-induced changes in forest disturbance and vegetation. *Nature* 343, 51–53.
- Parsons, D.J., 1978. Fire and fuel accumulation in a giant sequoia forests. *J. For.* 76, 104–105.
- Parsons, D.J., 1981. The historical role of fire in the foothill communities of Sequoia National Park. *Madrono* 28, 111–120.
- Parsons, D.J., 1994. Prescribed fire: current status and future directions. *Park Sci.* 14, 26.
- Parsons, D.J., DeBenedetti, S.H., 1979. Impact of fire suppression on a mixed conifer forest. *For. Ecol. Manage.* 2, 21–33.
- Pastor, J., Post, W.M., 1986. Influence of climate, soil moisture, and succession on forest carbon and nitrogen cycles. *Biogeochemistry* 2, 3–27.
- Pickett, S.T.A., White, P.S., 1985. *The Ecology of Natural Disturbance and Patch Dynamics*. Academic Press, New York.
- Pitcher, D.C., 1987. Fire history and age structure in red fir forests of Sequoia National Park, California. *Can. J. For. Res.* 17, 582–587.
- Prentice, I.C., 1992. Climate change and long-term vegetation dynamics. In: Glenn-Lewin, D.C., Peet, R.K., Veblen, T.T. (Eds.), *Plant Succession: Theory and Prediction*. Chapman and Hall, London, pp. 293–339.
- Rothermel, R.C., 1972. A mathematical model for predicting fire spread in wildland fuels. USDA For. Serv. Res. Paper INT-115.
- Rothermel, R.C., 1983. How to predict the spread and intensity of forest and range fires. USDA For. Serv. Gen. Tech. Report INT-143.
- Rundel, P.W., Parsons, D.J., Gordon, D.T., 1977. Montane and subalpine vegetation of the Sierra Nevada and Cascade ranges. In: Barbour, M.G., Major, J. (Eds.), *Terrestrial Vegetation of California*. Wiley, New York, pp. 559–599.
- Running, S.W., Nemani, R., Hungerford, R.D., 1987. Extrapolation of meteorological data in mountain terrain, and its use for simulating forest evapotranspiration and photosynthesis. *Can. J. For. Res.* 17, 472–483.
- Ryan, K.C., Reinhardt, E.D., 1988. Predicting postfire mortality of seven western conifers. *Can. J. For. Res.* 18, 1291–1297.
- Skinner, C.N., Chang, C., 1996. Fire regimes, past and present. In: *Sierra Nevada Ecosystem Project: Final report to Congress*, vol. 11, ch. 41. Davis: University of California, Centers for Water and Wildland Resources.
- Stephens, S.L., 1995. Effects of prescribed and simulated fire and forest history of giant sequoia (*Sequoiadendron giganteum* [Lindley] Buchholz.)-mixed conifer ecosystems of the Sierra Nevada, California. Ph.D. dissertation. University of California, Berkeley, CA.
- Stephenson, N.L., 1988. Climatic control of vegetation distribution: the role of the water balance with examples from North America and Sequoia National Park, California. Ph.D. dissertation. Cornell University, Ithaca, NY.
- Stephenson, N.L., 1990. Climatic control of vegetation distribution: the role of the water balance. *Am. Nat.* 135, 649–670.
- Stohigren, T.J., 1988. Litter dynamics in two Sierran mixed conifer forests. 1. Litterfall and decomposition rates. *Can. J. For. Res.* 18, 1127–1135.
- Swetnam, T.W., 1993. Fire history and climate change in giant sequoia groves. *Science* 262, 885–889.
- Turner, M.G., Gardner, R.H., Dale, V.H., O'Neill, R.V., 1989. Predicting the spread of disturbance across heterogeneous landscapes. *Oikos* 55, 121–129.
- Turner, M.G., Romme, W.H., 1994. Landscape dynamics in crown fire ecosystems. *Landscape Ecol.* 9, 59–77.
- Turner, M.G., Romme, W.H., Gardner, R.H., O'Neill, R.V., Kratz, T.K., 1993. A revised concept of landscape equilibrium: disturbance and stability on scaled landscapes. *Landscape Ecol.* 8, 213–227.
- Urban, D.L., Shugart, H.H., 1992. Individual-based models of forest succession. In: Glenn-Lewin, D.C., Peet, R.K., Veblen, T.T. (Eds.), *Plant Succession: Theory and Prediction*. Chapman and Hall, London, pp. 249–292.
- Urban, D.L., Harmon, M.E., Halpern, C.B., 1993. Potential response of Pacific northwestern forests to climatic change, effects of stand age and initial composition. *Climatic Change* 23, 247–266.
- Urban, D.L., Bonan, G.B., Smith, T.M., Shugart, H.H., 1991. Spatial applications of gap models. *For. Ecol. Manage.* 42, 95–110.
- Urban, D.L., Miller, C., Stephenson, N.L., Graber, D.M., 1998. Forest gradient response in Sierran landscapes: the physical template (in review).
- Vankat, J.L., 1982. A gradient perspective on the vegetation of Sequoia National Park, California. *Madrono* 29, 200–214.
- Vankat, J.L., 1985. General patterns of lightning ignitions in Sequoia National Park, California. In: Lotan, J.E., Kilgore, B.M., Fischer, W.C., Mutch, R.W. (Tech coord.). *Proc. Symp. Workshop on Wilderness Fire*. USDA For. Serv. Gen. Tech. Rep. INT-185, pp. 408–411.
- Vankat, J.L., Major, J., 1978. Vegetation changes in Sequoia National Park, California. *J. Biogeogr.* 5, 377–402.

- Van Wagner, C.E., 1973. Height of crown scorch in forest fires. *Can. J. For. Res.* 3, 373–378.
- van Wagtenonk, J.W., 1972. Fire and fuel relationships in mixed conifer ecosystems of Yosemite National Park. Ph.D. dissertation, University of California, Berkeley, CA.
- van Wagtenonk, J.W., 1983. Fire suppression effects on fuels and succession in short fire-interval wilderness ecosystems. In: *Proc. Symp. Workshop on Wilderness Fire*, Missoula MT, November 15–18, 1983. USDA For. Serv. Gen. Tech. Rep. INT 182, pp. 119–126.
- van Wagtenonk, J.W., 1985. The role of fire in the Yosemite wilderness. In: *Proceedings of the National Wilderness Research Conference*. USDA For. Serv. Gen. Tech. Rep. INT-212, pp. 2–9.
- van Wagtenonk, J.W., 1991. The evolution of National Park Service fire policy. *Fire Manage. Notes* 52, 10–15.
- van Wagtenonk, J.W., 1993. Spatial patterns of lightning strikes and fires in Yosemite National Park. In *12th Conf. Fire and Forest Meteorology*, Jekyll Island, GA, October 26–28, 1993, pp. 223–231.
- van Wagtenonk, J.W., Benedict, J.M., Sydoriak, W.M., 1996. Physical properties of woody fuel particles of Sierra Nevada conifers. *Int. J. Wildland Fire* 6, 117–124.
- van Wagtenonk, J.W., Benedict, J.M., Sydoriak, W.M., 1998. Fuel bed characteristics of Sierra Nevada conifers. *West. J. Appl. For.* 13, 73–84.
- van Wagtenonk, J.W., Sydoriak, C.A., 1987. Fuel accumulation rates after prescribed fires in Yosemite National Park. In *9th Conf. Fire and Forest Meteorology*, San Diego, CA, April 21–24, 1987, pp. 101–105.
- Waring, R.H., Schlesinger, W.H., 1985. *Forest Ecosystems: Concepts and Management*. Academic Press, Orlando.
- Waring, R.H., Schroeder, P.E., Oren, R., 1982. Application of the pipe model theory to predict canopy leaf area. *Can. J. For. Res.* 12, 556–560.
- Warner, T.E., 1980. Fire history in the yellow pine forest of Kings Canyon National Park. In: *Proceedings of the Fire History Workshop*, Tucson, AZ, October 20–24, 1980. USDA For. Serv. Gen. Tech. Rep. RM-81, pp. 89–92.